*Applied Mechanics and Materials* *Online: 2011-10-24*
*ISSN: 1662-7482, Vols. 110-116, pp 437-443*
*doi:10.4028/www.scientific.net/AMM.110-116.437*


# The Influence of different Turbulence Models on the FlowField Characteristics of an Aerospike Nozzle

S.Noori[1, a], A.Shahrokhi[2, b]

1Senior Researcher, Aerospace Research Institute, Ministry of Science, Research and Technology Tehran, Iran

[2]Senior Researcher, Aerospace Research Institute, Ministry of Science, Research and Technology, Tehran, Iran

[a]e-mail: noori@aut.ac.ir

[b]e-mail: shahrokhi@aut.ac.ir

**Keywords-**Aerospike nozzle, Turbulent, Thrust

**Abstract—**To improve the calculation of the flow properties of an aerospike nozzle, different turbulent models are studied in this research. The primary shape of the nozzle and the plug is determined through utilizing an approximate method. The flow field is then simulated using Navier-Stokes equations for compressible flow. The computational methodology utilizes steady state density-based formulation and a finite volume cell centered scheme to discretize the flow field equations. To accelerate the solution convergence, the flow field is divided into several zones. Each zone is facilitated with proper unstructured grid and appropriate initial conditions are implemented to each zone. The accuracy and the robustness of wall function based turbulence models i.e. standard and RNG k-ε models are compared with those of Spalart-Allmaras (S-A) and k-ω turbulence models.

## Introduction

The aerospike engine which is one of the altitude compensating nozzle engines, maintains its aerodynamic efficiency across a wide range of altitudes through using an aerospike plug.

Experimental research on aerospike nozzle and the parametric study was performed by Japanese in mid 90's [1-3]. Further research was carried out using the linear aerospike nozzle and the basic characteristics of the aerospike nozzle were obtained [4-6]. In Europe, the Future European Space Transportation Investigations Program for European Space Agency activated the research on such nozzles in 1998 [7,8].

In conventional convergent nozzles, the gas expansion process within the nozzle is largely controlled by the ambient pressure (or back pressure) of the surrounding air which is directly proportional to the nozzle altitude. In theory, the optimal thrust for a given jet or rocket engine occurs when the nozzle exit pressure equals surrounding pressure. With other design variables (mainly the combustion chamber pressure) fixed, there exists only one area ratio of exit area to throat area at a given altitude for optimal expansion in conventional nozzles. Compared to the conventional bell nozzles, unbounded expansion of the jet provides overall better performance in Aerospike nozzles.

In the aerospace literature it has been documented that the flow in supersonic nozzles is substantially influenced by viscous effects which reduce the performance of the propulsion system [9,10]. In many cases, the Reynolds number of the flow over the plug is high enough to oblige a turbulence flow along the nozzle spike. Koutsavdis applied several turbulence models for the computation of a plug nozzle flow field and compared the results with experimental observations. According to Koutsavdis studies about the influence of the flow separation around the boot tail of the truncated nozzle, the k-ω turbulence model appears to be the model of choice for prediction of most of the characteristics of the flow on the full nozzle.

The focus of the present study is on the flow field computation of an Aerospike nozzle using different turbulent models in order to provide some insight into the efficiency of each method on the accuracy of the nozzle thrust and pressure distribution estimations.

**Geometry of the plug nozzle**

In this section, an approximate method [11], has been used to design the central plug of the aerospike nozzle. The approximate method utilizes ideal rocket assumptions to derive a set of analytical relations, which can be used to calculate radius and flow properties at each longitudinal station of the plug of an aerospike nozzle [11-13]. The method can be summarized as following.

The expansion ratio for given values of combustion chamber pressure and optimum working altitude are calculated using the following relation.

$$\frac{A_t}{A_e}=\left(\frac{\gamma+1}{2}\right)^{\frac{1}{\gamma-1}}\left(\frac{P_e}{P_1}\right)^{\frac{1}{\gamma}}\left[\left(\frac{\gamma+1}{\gamma-1}\right)\left(1-\left(\frac{P_e}{P_1}\right)^{\frac{\gamma-1}{\gamma}}\right)\right]^{1/2} \tag{1}$$

The nozzle throat and the exhaust areas for a given value of the optimum thrust are determined through equation (2).

$$C_F=\left[\frac{2\gamma^2}{\gamma-1}\left(\frac{2}{\gamma+1}\right)^{\frac{\gamma+1}{\gamma-1}}\left(1-\left(\frac{P_2}{P_1}\right)^{\frac{\gamma-1}{\gamma}}\right)\right]^{1/2}=\frac{F}{A_t P_1} \tag{2}$$

$$A_e=\varepsilon A_t \tag{3}$$

The exhaust Mach number for a given expansion ratio is calculated using equation (4).

$$\frac{A_e}{A_t}=\frac{1}{M_e}\left[\frac{1+\frac{\gamma-1}{2}M_e^{\,2}}{1+\frac{\gamma-1}{2}}\right]^{\frac{\gamma+1}{2(\gamma-1)}} \tag{4}$$

For the exhaust flow to be parallel to the nozzle's axis, the throat must have an angle equal to the Prandtl-Meyer expansion angle corresponding to the exhaust Mach number: [14]

$$\theta_t=\nu(Me)=\sqrt{\frac{\gamma+1}{\gamma-1}}\tan^{-1}\sqrt{\frac{\gamma-1}{\gamma+1}\left(M_e^2-1\right)}-\tan^{-1}\sqrt{M_e^2-1} \tag{5}$$

The radius of the plug at throat is determined through the following equation.

$$A_t=\frac{\pi\left(r_e^{\,2}-r_t^{\,2}\right)}{\mathrm{Cos}\theta_t} \tag{6}$$

The local flow angle and local area for each station along the plug, which corresponds to a Mach number between 1 and $M_e$, are obtained.

$$\mu=\mathrm{Sin}^{-1}\frac{1}{M},\ \nu=\nu(M),\theta=\theta_t-\nu$$
$$\frac{A}{A_t}=\frac{1}{M}\left[\frac{2}{\gamma+1}\left(1+\frac{\gamma-1}{2}M^2\right)\right]^{\frac{\gamma+1}{2(\gamma-1)}} \tag{7}$$

The local radius (r) of plug and longitudinal coordinate (x) at the same station are calculated using the following equations.

$$r^2=r_e^{\,2}\left(1-\frac{A}{A_t}\frac{\mathrm{Sin}(\mu+\theta)}{\mathrm{Sin}\mu\mathrm{in}\mu\ \theta_t}\right) \tag{8}$$

$$x=\frac{r_e-r}{\tan(\mu+\theta)} \tag{9}$$

The calculation of the local flow angle, local area for each station along the plug, the local radius (r) of plug and longitudinal coordinate should be repeated incrementally from M=1 to M=$M_e$ to obtain coordinates for the entire plug. The entire nozzle geometry is shown in Figure 1.

The method presented in this section is implemented to the design an aerospike nozzle in the 4-5 KN thrust class with the specifications originally introduced in [14]. The chamber pressure is

2067857 N/m$^2$ and the optimum design altitude is 3657.6 m in which the optimum thrust of 4443.9 N is achieved. The specific impulse and mass flow rate are 235 s and 3.25758 kg/s respectively. The propellant is ethanol- oxygen with the specific heat ratio of 1.21 and $C_P$ = 1286.68 J/kgK.

The nozzle specifications are calculated using the relations presented in this section. The obtained values for the throat angle and the throat radius are equal to57.1665° and 0.045221 m respectively. The estimate exhaust Mach number and exhaust radius are 2.80434 and 0.047888 m respectively.

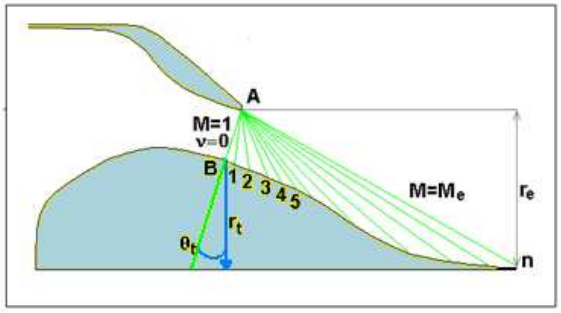


Figure 1. Schematic of the axisymmetric aerospike nozzle

## Calculation of aerospike nozzle thrust

One of the most suitable criteria for measuring the performance of a nozzle is the thrust of the propulsion system. A plug nozzle thrust force includes three terms.

Exhaust momentum thrust of the convergent part of the nozzle which is the integral of the momentum over the throat area and is determined through the following equation.

$$F_1 = \int (\rho V dA) V_x \tag{10}$$

The pressure thrust of the nozzle throat area is the second term which is obtained using equation (11).

$$F_2 = \int (P - P_{atm}) \mathrm{Cos}\theta_t dA \tag{11}$$

The third component is the force exerted to the entire plug surface and is calculated from the equation bellow.

$$F_3 = \int (P - P_{atm}) \mathrm{Sin}\theta_t dA \tag{12}$$

The total thrust force is achieved putting the three parts together.

## Numerical method

The numerical analysis of internal and external flow of the aerospike nozzle is performed using Navier-Stokes equations considering turbulent flow. The computational methodology utilizes a steady state density-based formulation and a finite volume cell centered scheme to discretize the flow field equations. The flow field is divided into several zones to facilitate each zone having the proper unstructured grid and also to offer appropriate initial conditions for each zone to accelerate the solution convergence. The grid density increases towards the throat and the remaining computational domain coarseness increases outward from the nozzle outlet.

Different methods are employed to model the turbulent boundary layer. Spalart-Allmaras (S-A) one equation model, is one of the method used for turbulence modeling. In comparison with one equation turbulence models, two equation turbulence models are complete, i.e., they can be used to predict the properties of a given turbulence flow with no prior knowledge of turbulence structure. Based on the physical specifications of the flow, three two-equation turbulent models i.e. standard and RNG k-ε models and k-ω turbulence models are applied. More information about different turbulence models can be found in [15].

**Results and discusions**

This section describes numerical modeling and analysis of internal and external flow of the aerospike nozzle introduced in section II. The results presented in this section are obtained using a commercial CFD code. The objective of the analysis is the comparison of the thrust calculated employing Navier-Stokes equations and different turbulence models. The inlet properties of the convergent part considered here are:

$L=0.2$ m

$A_i = 7.212855\times10^{-3}$ m$^2$

$A_i/A_t = 5.01384$

$M_i = 0.13$

$P_i = 0.98984$

$P_0 = 2045430$ N/m$^2$

The solution domain has been divided into 4 regions to provide the solution domain with different initial conditions defined in each region. Considering the axial symmetry of the problem, numerical solution is carried out in half of the entire domain, bounded by the symmetry line. Figure 2 shows the grid distribution in the convergent part of the nozzle and near the plug. To meet the requirement for the $Y^+$ parameter in different turbulence modeling, the grid coarseness is modified near the wall for each turbulence model, resulting in the total number of 149644, 166537 and 191097 cells for k-ε, Spalart-Almaras and k-ω models respectively.

The Average properties of combustion products resulting from chemical reaction of ethanol and oxygen is assumed for the entire fluids in all regions. The boundary condition at the inlet of the convergent section

is the specified mass flow of 3.25757 kg/s with the total temperature of 1577.826 K. The main characteristic of the exhaust flow of the aerospike nozzle is the formation of a series of expansion waves, emanating from the upper lip of the convergent part of the nozzle. In contrary to conventional nozzles, the exhaust flow is not limited to a solid wall. So in the case of a plug the expansion waves can adjust their intensity and domain to match with the external flow.

The pressure and Mach number contours are illustrated in Figures 3 and 4 using Standard k-ε turbulence model. As seen in this figure, the domain covered by the expansion waves ends before the end of the plug. In order to adapt to the external flow, the flow over the plug is continued by the compression waves which increase the pressure and reduce Mach number to a value close to that of the ambient. The convergent nozzle first cell $Y^+$ value for Standard k-ε turbulence model are shown in Figure 5. The $Y^+$ values are limited to about 250 which is acceptable due to using wall

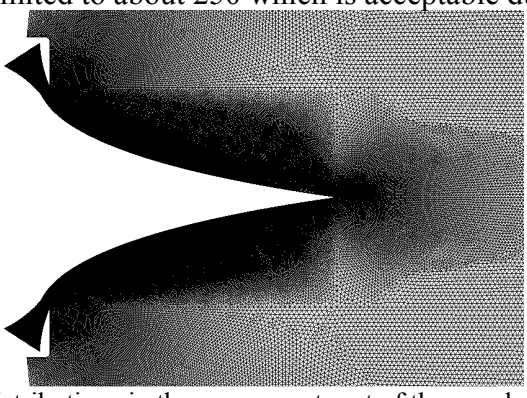

Figure 2. Grid Distributions in the convergent part of the nozzle and along the plug

function in the viscous sublayer near the wall.

Figures 6 and 7 demonstrate the pressure and Mach number contours for RNG k-ε turbulence model. The results are similar to the ones obtained through using standard k-ε turbulence model. First cell $Y^+$ distribution over the convergent nozzle wall for RNG k-ε model is presented in Figure 8. The maximum $Y^+$ value is less than 300 which is within the satisfactory range.

The pressure and Mach number contours for k-ω turbulence model are shown in Figures 9 and 10. The contours in both figures are significantly similar to the ones in k-ε turbulence model cases. First cell $Y^+$ values distribution is provided in Figure 11 in the case of k- ω turbulence model. In the

case of k- ω model, the mesh is refined until the average $Y^+$ of about 100 is obtained. Since a finer mesh would remarkably increase the number of cells, a wall function is used for viscous sublayer region of the boundary layer.

Figures 12 and 13 illustrates the pressure and Mach number contours for the case that Spalart-Almaras turbulence model is employed. The results are slightly different with other three methods. $Y^+$ values for the convergent nozzle wall are show in Figure 14. First cell $Y^+$ values are kept less than 50 to meet the near wall conditions in this case. To realize the influence of the turbulence modeling in the flowfield properties, the flow is resolved considering laminar boundary layer. The pressure and Mach contours are shown in Figures 15 and 16 respectively. In comparison with the turbulent cases, the expansion and compression waves are stronger in this case.

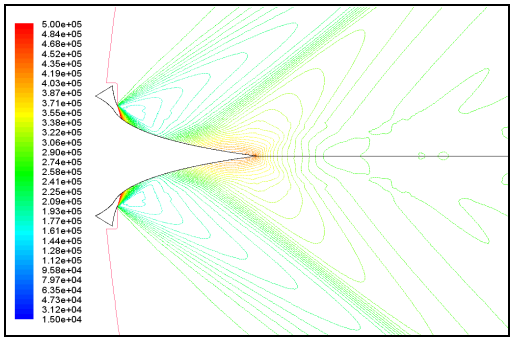

Figure 3. Contours of static pressure, standard k-ε;

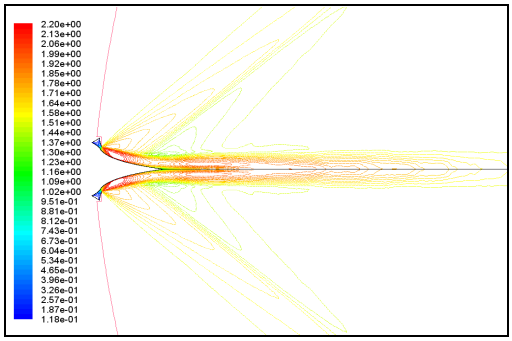

Figure 4. Contours of Mach number, standard k-ε

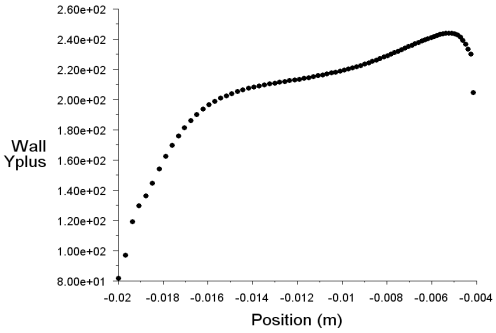


Figure 5. Convergent nozzle wall Y+ Curve, standard k-ε

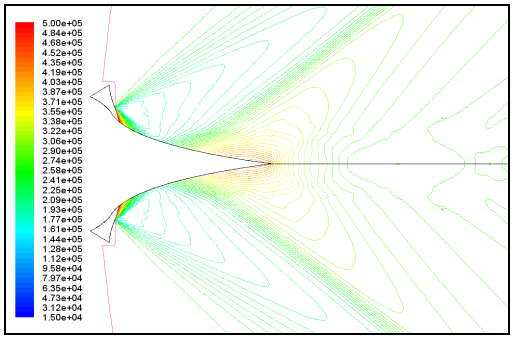

Figure 6. Contours of static pressure, RNG k-ε

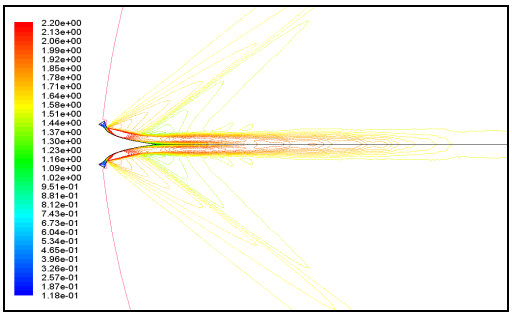

Figure 7. Contours of Mach number, RNG k-ε

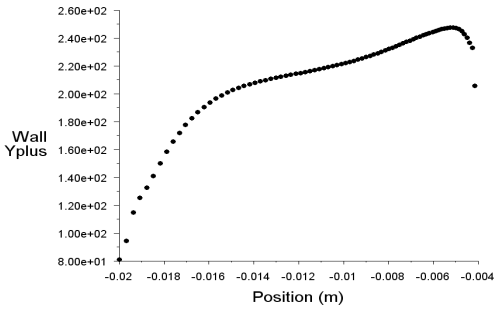


Figure 8. Convergent nozzle wall Y+ Curve, RNG k-ε

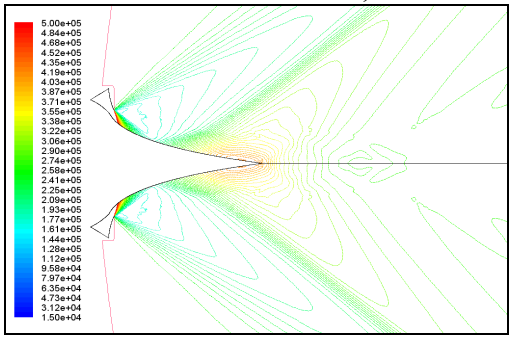

Figure 9. Contours of static pressure, k-ω

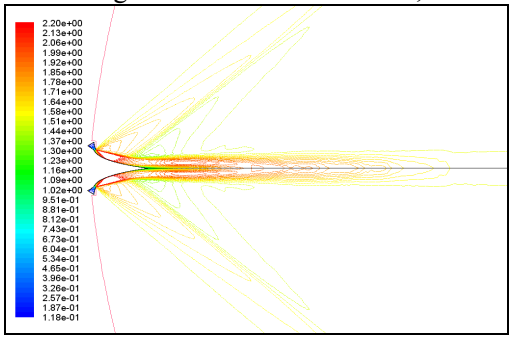

Figure 10. Contours of Mach number, k-ω

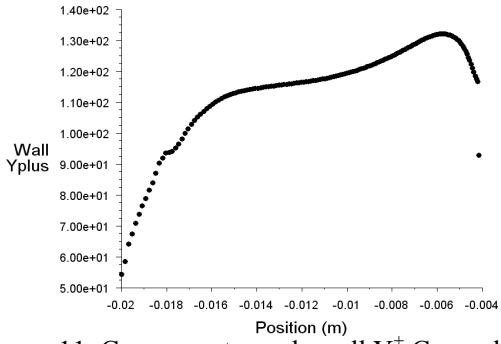


Figure 11. Convergent nozzle wall $Y^+$ Curve, k-ω

Three thrust components mentioned in Section III and the total thrust forces are tabulated in Table I. The results are remarkably different when turbulence model is employed in the numerical calculations. Thrust force calculated using Standard K-ε differs slightly with other cases.

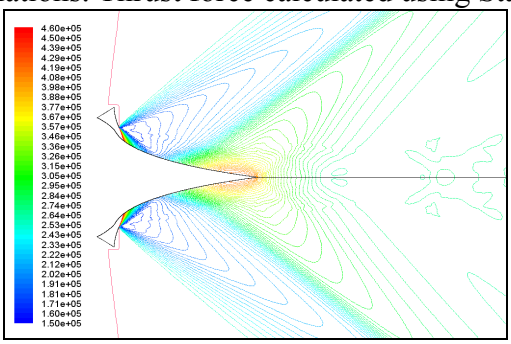

Figure 12. Contours of static pressure, Spalart-Almaras

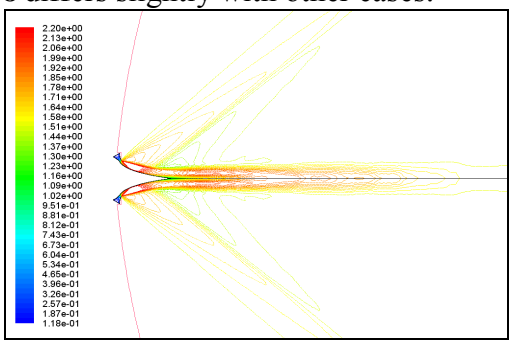

Figure 13. Contours of Mach number, Spalart-Almaras

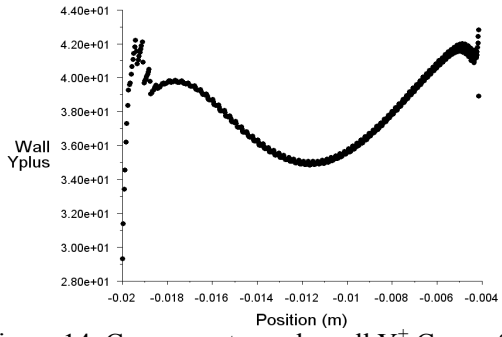


Figure 14. Convergent nozzle wall $Y^+$ Curve, Spalart-Almaras

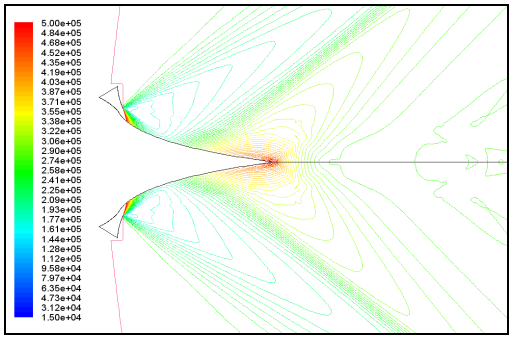

Figure 15. Contours of static pressure, Laminar

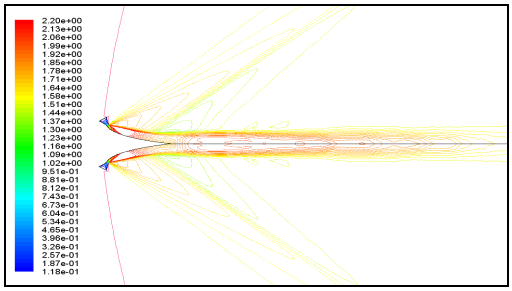

Figure 16. Contours of Mach number, Laminar

TABLE I. Thrust of the aerospike nozzle in different Flow Solver Model

| Flow Solver Model | T1 | T2 | T3 | Total Thrust |
|---|---|---|---|---|
| Laminar | 1450.50 | 993.54 | 919.52 | 3363.56 |
| K-ω | 1480.03 | 991.96 | 811.87 | 3283.86 |
| K-ε (standard) | 1453.27 | 986.14 | 809.78 | 3249.18 |
| K-ε (RNG) | 1479.14 | 974.64 | 818.56 | 3272.35 |
| Spalart-Almaras | 1483.08 | 978.26 | 813.52 | 3274.85 |

**References**

[1] T.Ito, K. Fujii and A.K. Hayashi, “Computations of the Axisymmetric Plug Nozzle Flow Fields, ”AIAA Paper 99-3211, 1999.

[2] T. Tomita, H. Tamura, and M. Takahashi, “An Experimental Evaluation of Plug Nozzle Flow Fields, ”AIAA Paper 96-2632, 1996.

[3] T.Tomita, M. Takahashi and H. Tamura, “Flow Field of Clustered Plug Nozzles, ” AIAA Paper 97-3219, 1997.

[4] T. Tomita, M. Takahashi , T. Onodera, and H. Tamura, “Effects of Base Bleed on Thrust Performance of a Linear Aerospike Nozzle, ”AIAA Paper 99-2586, 1999.

[5] T. Onodera, T. Tomita, and H. Tamura, “Numerical Investigation of the Flow Field around Linear Aerospike Nozzles,” AIAA Paper 99-2588, 1999.

[6] H. Sakamoto, M. Takahashi , M. Sasaki, T. Tomita, K. Kusaka, and H. Tamura, “An Experimental Study on a 14kN Linear Aerospike Nozzle Combustor, ” AIAA Paper 99-2761,1999.

[7] D. Vuillamy, and V. Duthoit, “European Investigation of Clustered Plug Nozzles, ” AIAA Paper 99-2350, 1999.

[8] G. Hagemann, H. Immich, and M. Terhardt, “Flow Phenomena in Advanced Rocket Nozzles – The Plug Nozzle ,” AIAA Paper 98-3522, 1998.

[9] J.J. Korte, A. O. Salas, H.J. Dunn, N.M. Asexandrov, W.W. Follett, G.E. Orient, and A.H. Hadid, “ Multidisciplinary Approach to Linear Aerospike Nozzle Optimization, ” AIAA Paper 97-3374, 1997.

[10] J.J. Korte, “Parametric Model of an Aerospike Rocket Engine, ”AIAA Paper 2000-1044, 2000.

[11] G. Angelino, “Approximation Method for Plug Nozzle Design, ” AIAA Journal, Vol. 2, No. 10, Oct. 1964, pp. 1834-1835.

[12] H. Greer, “ Rapid Method for Plug Nozzle Design,” ARS Journal, April 1971, pp. 560-561.

[13] G. P. Sutton, O. Biblarz, “Rocket Propulsion Elements, ” 7th Edition, John Wiley & Sons, Inc., 2000.

[14] E. Besnard, H. H. Chen, T. Mueller and J. Garvey, “Design, Manufacturing and Test of a Plug Nozzle Rocket Engin, ” AIAA Paper 02-4038, 2002.

[15] D. C. Wilcox, “Turbulence Modeling for CFD, ” Third edition, DCW Industries,2006.